Egyptian Journal of Radiology and Nuclear Medicine

RESEARCH

Open Access

Contributional role of susceptibility-weighted imaging and apparent diffusion coefficient in pediatric brain tumor grading

Ahmed S. Abdelrahman*, Mena E. Y. Ekladious and Nivan Hany Khater

Abstract

Background: Central nervous system neoplasms are a primary cause of mortality and one of the most frequent solid tumors in children. Magnetic resonance imaging (MRI) plays a key role in the diagnosis and treatment response of pediatric brain tumors as well as providing us with functional information regarding cellularity, metabolism, and neoangiogenesis. This study aimed to evaluate the contributional role of susceptibility-weighted imaging (SWI) and diffusion weight imaging (DWI) in pediatric brain tumor grading by assessing the intratumoral susceptibility signals (ITSS), apparent diffusion coefficient (ADC), and relative ADC (rADC).

Results: A significant correlation was noted between the (ITSS) score and the brain tumor grade ($P<0.001$) with a descending trend in the low-grade tumor (ITSS score 0 = 14/29, score 1 = 11/29, and score 2 = 4/29) and an ascending trend in the high-grade tumor (ITSS score 0 = 4/41, score 1 = 9/41 and score 2 = 22/41). No embryonal tumor showed an ITSS score of 0. Apparent diffusion coefficient sensitivity and specificity were 82.9% and 82.8%, respectively, while rADC sensitivity and specificity were 91.4% and 86.2%, respectively. For high-grade tumors, the ITSS score 2 had a significant positive prediction ($P=0.009$) and the rADC value had a significant negative prediction ($P=0.031$).

Conclusions: Susceptibility-weighted imaging ITSS score, ADC, and rADC have a promising role in preoperative pediatric brain tumor grading and should be considered as complementary sequences to routine MRI studies.

Keywords: MRI, ADC, Brain neoplasms, Pediatric

Background

Magnetic resonance imaging (MRI) has a crucial preoperative role in intracranial tumors as regards detection, grading, putting a differential diagnosis, guiding for biopsy as well as in treatment decision planning [1]. The most frequent solid tumors in the pediatric age-group are brain neoplasms with a five-year survival rate of 73.6% among children under 18 years old, depending on the genetic, molecular, and histologic characteristics of the tumor [2].

High-grade brain lesions are treated differently than low-grade lesions, hence the importance of grading the lesion accurately for proper therapy and for assessing the prognosis [3]. Stereotactic biopsy is commonly taken to help differentiate between both; however, pathologic microvascularity is not uniform within the lesion and the biopsy taken does not include all portions of the malignant tumor (4). Susceptibility-weighted imaging is an important noninvasive tool that can assess the internal architecture and degree of microvascularity of the whole lesion using intratumoral susceptibility signals (ITSS) [5].

*Correspondence: dr_ahmedsamy@yahoo.com; ahmedsamy@med.asu.edu.eg

Radiology Department, Faculty of Medicine, Ain Shams University, Cairo, Egypt

ITSS is defined as low-signal-intensity dot-like or linear structures confluent or non-confluent within the tumor and not obvious on the conventional MR images [6]. The role and capabilities of SWI in pediatric brain tumors have barely been evaluated with only one study assessing the true value of ITSS in the young age-group [7].

Susceptibility-weighted imaging has the unique ability to detect differences in tissue susceptibility, easily enhancing the contrast between vessels and adjacent brain parenchyma. To create a strong enhanced image, phase images are combined with magnitude images, thereby enabling the identification and differentiating between calcifications, neoangiogenesis, and microhemorrhages within the tumor [8, 9].

Pathological criteria for grading tumors include not only vascularity but also cellularity and degree of cellular proliferation; therefore, the combination of different imaging modalities can provide us with complementary information and increase the diagnostic accuracy (10). The degree of tumor cellularity has been correlated with the apparent diffusion coefficient (ADC) value [11]. The apparent diffusion coefficient is derived from diffusion-weighted imaging (DWI), which detects microscopic changes in the tumor and provides an idea of the movement of intracellular and extracellular water molecules in biological tissue. ADC is negatively correlated with the degree of proliferation and cell density [12–14]. Relative ADC, on the other hand, is measured as the ratio of ADC values between the solid portion of the tumor and adjacent normal-appearing white matter or the contralateral white matter [15].

The aim of this study was to evaluate the usefulness and added value of ITSS score, ADC, and r ADC in the preoperative grading of pediatric brain tumors.

Methods

Patients

This prospective study was conducted in our institution from October 2020 to September 2021, following ethical committee approval and with written informed consent taken from the children's guardians. The study included 64 children who underwent brain MRI study with SWI and DWI. There were 35/64 (54.7%) males and 29/64 (45.3%) females, with a median age of 10 years (range 0.5 to 17 years). Astrocytoma, neuronal and mixed glioneuronal tumors, embryonal tumors, ependymoma, and a few other tumors were the five groups of low and high-grade brain tumors that were identified and confirmed by neuropathologists according to the World Health Organization classification of tumors of the central nervous system 2016. Each group contained a variety of tumor types and grades, ranging from low- to high-grade lesions.

Exclusion criteria included children with a history of surgery/prior excision or local treatment or those who received radiotherapy or chemotherapy before MRI. Also, those with a contraindication to MRI, e.g., metallic implant, or cannot be given IV contrast (gadopentetate dimeglumine) as those with allergy or renal impairment. Inclusion criteria were children in stable clinical condition without any known contraindications to MR imaging or intravenous application of standard MR imaging contrast agents.

Technique of MRI

The MRI study was carried out on a 1.5 T machine (Philips Ingenia) with a dedicated head coil. If the patient was old enough, he or she was asked to lie supine, head-first, and to breathe quietly. Thirty-two patients in this study were given sedative medications; their vital signs were monitored throughout the procedure. Contrast-enhanced MRI examination was done for all patients which included axial T1WI, T2WI, FLAIR, and post-contrast axial, sagittal, and coronal T1 WI sequences with 230×182 mm FOV, 5 mm slice thickness. T1WI: (TR/TE: 450/12), T2WI: (TR/TE: 3500/100), FLAIR: (TR: 9000, TE: 120). DWI was performed using a single-shot echo-planar imaging sequence with the following parameters: TR/TE: 3960/115 ms, 2 number of excitations, flip angle = 90°, and 5 mm slice thickness. ADC maps were generated from DWI (b value 0 and 1000 s/mm^2). SWI parameters were as follows: TR/TE 52/12 ms, flip angle 10°, slice thickness 2 mm, and matrix 256×256. A minimum intensity projection (minIP) image was used to display the combined processed data using contiguous sections of thickness 16 mm using 8 contiguous 2 mm slices in the axial plane.

Image analysis

The MR system's SWI post-processing software was used to generate corrected-phase and magnitude images. The susceptibility effects were identified on the magnitude images as foci of hypointensity in the tumor, and in this study, the ITSS was referred to as both hemorrhagic and hypervascular tumor components appearing as dot-like or linear foci. Calcific foci were identified as bright foci in the phase images and were subsequently subtracted from the total number of ITSS. The SWI images were independently interpreted by two neuroradiologists with 7 and 10 years of experience (ME, NH, respectively) blinded to the histopathological results. ITSS score was evaluated as follows: 0; no ITSS, 1; 1 to 10 ITSS and 2; more than 10 ITSS [16–18]. In cases of disagreement between both readers, the final ITSS score was reached by consensus.

The ADC value was determined by placing regions of interest (ROI) over the solid portion of the tumor in

the generated ADC maps, avoiding cystic, necrotic, and hemorrhagic regions. rADC was calculated as the ratio of the solid portion of the tumor's ADC to the contralateral normal white matter.

Statistical analysis

Data were analyzed using Statistical Package for Social Science (IBM Corp. Released 2017. IBM SPSS Statistics for Windows, Version 25.0. Armonk, NY: IBM Corp.). Parametric quantitative data were expressed as mean ± standard deviation (SD). Median and range were used to report the nonparametric quantitative data. Qualitative data were described as frequency and percentage. Kendall's tau b (τb) test was used to measure the strength and direction of association (trend) between ITSS score and brain tumor grade. Independent samples t test was used to compare the means of ADC and rADC in low and high-grade tumor groups. Intraclass correlation (ICC) was used to determine the inter-reader agreement of continuous variables. The inter-reader agreement of the categorical variables was determined using Cohen's kappa coefficient (K). Receiver operator characteristic (ROC) curve analysis was performed to determine the optimal cutoff value. Multinomial logistic regression models using enter method were reconstructed to specify the optimal predicting variables for high-grade tumors. P value < 0.05 was considered statistically significant.

Table 1 Demographic and radiological data of the study population

Age (year)[a]	**10 (0.5–17)**
Gender[b]	
Female	35 (54.7%)
Male	29 (45.3%)
Tumor grade[b]	
Low-grade	29 (45.3%)
High-grade	35 (54.7%)
Histopathological tumor subgroup[b]	
Astrocytomas	33 (51.6%)
Embryonal tumor	12 (18.7%)
Neuronal and mixed glioneuronal tumor	11 (17.2%)
Ependymomas	6 (9.4%)
Other	2(3.1%)
Localization[b]	
Supratentorial	41 (64.1%)
Infratentorial	23 (35.9%)
Localization[b]	
Midline	22 (34.4%)
Off-midline	42 (65.6%)

[a] Median (range)

[b] Number (%)

Results

The current study included 64 children, 35/64 (54.7%) of whom were males and 29/64 (45.3%) were females, with a median age of 10 years (range 0.5 to 17 years). Out of the 64 patients 29 (45.3%) were low-grade tumors and 35 (54.7%) were high-grade tumors, which were divided as follows: 33 astrocytomas, 12 embryonal tumors, 11 neuronal and mixed glioneuronal tumors, 6 ependymomas, and 2 other tumors (one germinoma and one choroid plexus carcinoma). In terms of tumor location, 41/64 (64.1%) were supratentorial and 23 (35.9%) were infratentorial. Forty-two out of 64 (65.6%) were off-midline tumors and 22 (34.4%) were midline (Table 1).

Table 2 Correlation of ITSS score with different brain locations and subgroups

Tumor group (N)	**ITSS**			**τb[a]**	***P***
	0	**1**	**2**		
All tumor (64)				0.496	< 0.001*
Low grade	14 (48.3%)	11 (37.9%)	4 (13.8%)		
High grade	4 (11.4%)	9 (25.7%)	22 (62.9%)		
Supratentorial (41)				0.451	0.002*
Low grade	9 (45%)	8 (40%)	3 (15%)		
High grade	3 (14.3%)	5 (23.8%)	13 (61.9%)		
Infratentorial (23)				0.571	0.005*
Low grade	5 (55.6%)	3 (33.3%)	1 (11.1%)		
High grade	1 (7.1%)	4 (28.6%)	9 (64.3%)		
Off-midline (42)				0.496	0.001*
Low grade	8 (42.1%)	8 (42.1%)	3 (15.8%)		
High grade	2 (8.7%)	6 (26.1%)	15 (65.2%)		
Astrocytoma (33)				0.425	0.011*
Low grade	9 (47.4%)	7 (36.8%)	3 (15.8%)		
High grade	2 (14.3%)	4 (28.6%)	8 (57.1%)		
Neuronal and mixed glioneuronal tumor (11)				0.462	0.125
Low grade	5 (50%)	4 (40%)	1 (10%)		
High grade	0	0	1 (100%)		
Embryonal (12)				–	–
Low grade	–	–	–		
High grade	0	4 (33.3%)	8 (66.7%)		
Ependymoma (6)				–	–
Low grade	–	–	–		
High grade	1 (167%)	1 (16.7%)	4 (66.7%)		
Other (2)				–	–
Low grade	–	–	–		
High grade	1 (50%)	0	1 (50%)		

N = number

*Significant

[a] Kendall's tau b

In general, a significant strong association between the ITSS score and the tumor grade (τb = 0.496, $P < 0.001$) was noted with a descending trend in the low-grade tumor (ITSS score 0 = 14/29, score 1 = 11/29, and score 2 = 4/29), ad an ascending trend in the high-grade tumor (ITSS score 0 = 4/41, score 1 = 9/41 and score 2 = 22/41). A similar strong trend was also noted in the supratentorial, infratentorial, off-midline, and midline tumors (τb = 0.451, 0.571, 0.496, and 0.505, respectively, $P < 0.05$) (Table 2).

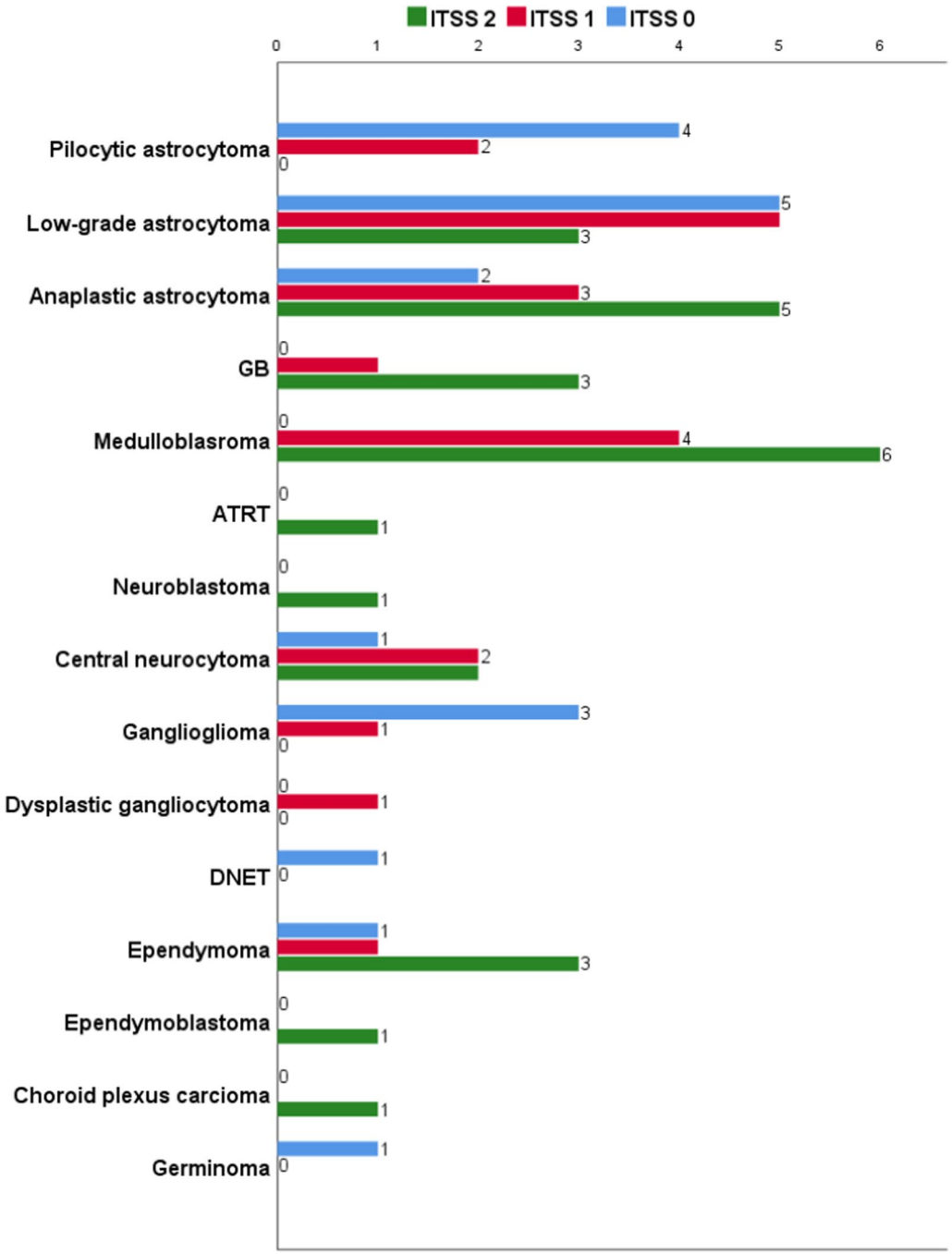

Fig. 1 Distribution of ITSS score in different pediatric brain tumor types. GB = glioblastoma, ATRT = atypical teratoid rhabdoid tumor, DNET = dysembryoplastic neuroepithelial tumor

Table 3 ADC and rADC of the low-grade and high-grade tumor

	Low grade		High grade		*P* value[a]
	Mean ± SD	Range	Mean ± SD	Range	
ADC ($\times 10^{-3}$ mm^2/s)	1.38 ± 0.25	0.95–1.9	0.88 ± 0.28	0.4–1.7	< 0.001*
rADC	1.64 ± 0.32	0.9–2.7	0.99 ± 0.32	0.55–1.7	< 0.001*
ADC contralateral	0.85 ± 0.11	0.71–1.05	0.9 ± 0.12	0.7–1.05	0.122

[a] Independent sample t test

*Significant

Among the astrocytoma groups, there was still a significant strong association between low-grade tumors and ITSS 0 and 1 and a strong association between high-grade tumors and ITSS score 2 (τb = 0.425, $P < 0.011$). On the other hand, no significant association was noted between the different grades of neuronal and mixed glioneuronal tumor and ITSS score ($P = 0.125$) (Table 2).

Pilocytic astrocytoma was either ITSS score 0 (4/6) or score 1 (2/6) and glioblastoma (GB) was score 2 (3/4) or score 1 (1/4). Score 0 was never seen in embryonal tumors, as medulloblastoma was either score 2 (6/10) or 1 (4/10) and both atypical teratoid rhabdoid tumor (ATRT) and central neuroblastoma were score 2. Ependymoma was either a score 2 (3/4) or a score 1 (1/4). Figure 1 shows the different brain tumor types and their associated ITSS scores.

The mean value of the ADC and rADC for the high-grade tumors was significantly lower than that of the low-grade tumors ($P < 0.001$) (Table 3), and the optimal cutoff value of the ADC for identification of high-grade tumor was 1.15×10^{-3} mm^2/s (AUC = 0.910 95% CI 0.0.840–0.981, $P < 0.001$) with an ADC sensitivity and specificity of 82.9% and 82.8%, respectively, while the optimal rADC cutoff value was 1.375 (AUC = 0.925, 95% CI 0.860–0.989, $P < 0.001$), with sensitivity and specificity of 91.4% and 86.2%, respectively (Table 4; Fig. 2).

An almost perfect inter-reader agreement was noted for the ITSS grade (K = 0.88, 95% CI 0.781–0.980, $P < 0.001$), ADC (ICC = 0.994, 95% CI 0.990–0.996, $P < 0.001$), and rADC (ICC = 0.995, 95% CI 0.993–0.997, $P < 0.001$).

A significant multinomial logistic regression model (P 0.001) involving ITSS score, ADC, and rADC was reconstructed with a model accuracy of 87.5%. ITSS score 2 had a significant positive prediction for high-grade tumor (B = 3.395), with an odds ratio of 29.812 ($P = 0.009$). The rADC value, on the other hand, had a negative significant prediction ($P = 0.031$) for high-grade tumors ($y = 10.193 + (\text{rADC} \times -6.211)$) (Table 5). The relationship between ITSS, ADC, rADC, and tumor grade is demonstrated in Figs. 3, 4, 5, 6, and 7.

Discussion

Many studies conducted on adults have shown that SWI can be used to evaluate intracranial tumors [19–21], with SWI detecting intratumoral vascularity and hemorrhage better than other MR sequences. It is very sensitive in detecting small vessels of the brain as it multiplies the phase mask with the magnitude images to enhance the venous data [22]. Our study is one of the few studies conducted on the pediatric patient group involving 64 children with brain tumors with an age range from 0.5 to 17 years (median 10 years). To our knowledge, one previous retrospective study evaluating the ITSS score in the pediatric group was performed by Gaudino et al. [7] and enrolled 96 pediatric patients with an age range from 1 to 16 years (median 9.6 years).

Among the astrocytoma groups in our study, glioblastomas (GB) were a score 2 (3/4) or a score 1 (1/4). This is in agreement with Hsu et al. [16] and Saini et al. [17]; both studies concluded that the highest ITSS scores are commonly seen with glioblastomas. On the other hand, Aboian et al. [23] reported ITSS score 0 in high-grade H3K27M-mutant diffuse midline gliomas with only two cases showing a score of 2, despite their heterogeneous histologic appearance with bleeding tendency and vascularity. Pilocytic astrocytoma (PA) was either score 0 (4/6) or score 1 (2/6); 2 cases showed a score 2 despite PA being low-grade tumors. According to Gaudino et al. [24], these high ITSS scores were likely because PAs tend to bleed and display abundant vascularity (described as "glomeruloid vessels").

Gaudino et al. [7] also reported that no medulloblastoma had an ITSS score of 0 and that the majority of ependymomas (3/4) had a score of 2. Gupta et al. [25] described a high cerebral blood volume and thus high

Table 4 Area under the curve and cutoff value of ADC and rADC for identification of high-grade tumor

	AUC	95% CI	*P* value	Cutoff value	Sensitivity (%)	Specificity (%)	PPV (%)	NPV (%)	Accuracy (%)
ADC	0.910	0.840–0.981	< 0.001*	≤ 1.15	82.9	82.8	85.3	80	82.8
rADC	0.925	0.860–0.989	< 0.001*	≤ 1.375	91.4	86.2	88.9	89.3	89.1

*Significant

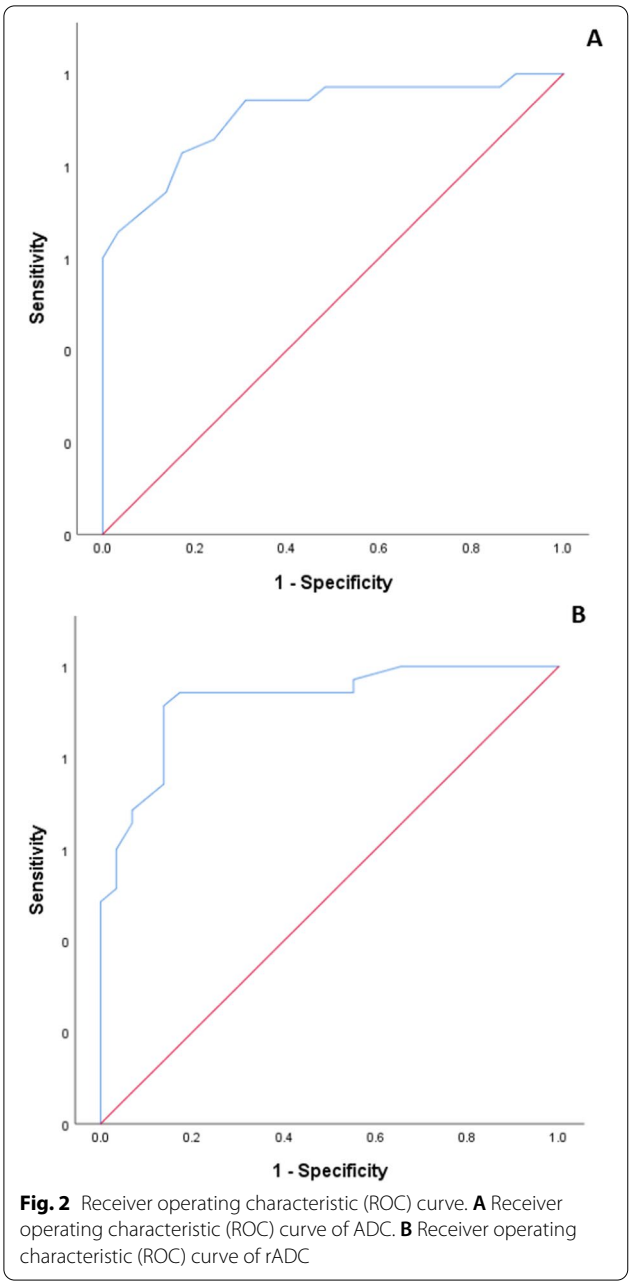

Fig. 2 Receiver operating characteristic (ROC) curve. **A** Receiver operating characteristic (ROC) curve of ADC. **B** Receiver operating characteristic (ROC) curve of rADC

Table 5 Multinomial logistic regression model for predicting high-grade tumor

	Odds ratio	95% CI	*P* value	*B*
Intercept	26,719	–	0.002*	10.193
ITSS (1)	0.691	0.085–5.652	0.730	− 0.369
ITSS (2)	29.812	2.297–386.896	0.009*	3.395
rADC	0.002007	0.000–0.563	0.031*	− 6.211
ADC	0.120	0.001–26.794	0.442	− 2.119

95% CI = 95% confidence interval

*Significant

perfusion and vascularization in ependymomas, thus the cause of multiple hypointense foci on SWI. In our study, medulloblastomas were either scored 2 (6/10) or 1 (4/10), while ATRT and central neuroblastoma were scored 2. Five cases of ependymoma were examined; 3 of which were a score 2 and one case a score 1, with only one case a score 0. The sample size was small, giving no explanation for this single case with score 0.

In our study, the ITSS score correlated relatively well with tumor grading within the category of mixed glioneuronal tumors. ITSS scores 0 and 1 were seen in 5/11 and 4/11 of the cases of the mixed glioneuronal tumors, respectively, with the exception of one low-grade and one high-grade central neurocytoma that had ITSS score of 2. Gaudino et al. (7) results did not correlate well, with a score of 2 assigned to 4/24 cases presenting with a variety of MRI features with variations in intratumoral bleeding. However, their experience with SWI in the assessment of DNET showed a high performance with an ITSS score of 0 which correlates well with their benign behavior.

We reported a single choroid plexus carcinoma case with an ITSS score of 2. However, in a study done by Lin et al. [26], SWI could not detect the signs of malignancy that characterized high-grade choroid plexus carcinomas as frequent invasion, necrosis, increased cellular density, and pleomorphism. This also is in keeping with a study done by Gaudino et al. [7] where an ITSS score of 2 was assigned to two papillomas and one carcinoma.

Our study revealed ITSS scores 1 and 2 in several low-grade tumors in the pediatric population despite the fact that many studies have shown that SWI high-grade gliomas in adults showed significantly higher ITSS scores than in low-grade gliomas or even the absence of ITSS in low-grade gliomas [1, 6, 15, 20].

In general, our prospective study showed a significant strong correlation between the ITSS score and the brain tumor grade ($P<0.001$) with an ITSS score descending trend in the low-grade tumors (ITSS score 0 = 14/29, score 1 = 11/29, and score 2 = 4/29) and an ascending trend in the high-grade tumors (ITSS score 0 = 4/41, score 1 = 9/41, and score 2 = 22/41).

Another factor other than the microvasculature contribution to the malignancy of tumors is cell density and degree of cellularity, with restricted diffusion favoring malignancy [27]; thus, we combined ADC and rADC in our study. The optimal cutoff value of the ADC for the identification of high-grade tumors was 1.15×10^{-3} mm^2/s, while the optimal rADC cutoff value was 1.375. The mean value of the ADC and rADC for the high-grade tumors was significantly lower than the low-grade tumors ($P<0.001$) which revealed sensitivity of 82.9% and 91.4%, respectively, and specificity of 82.8% and 86.2%, respectively.

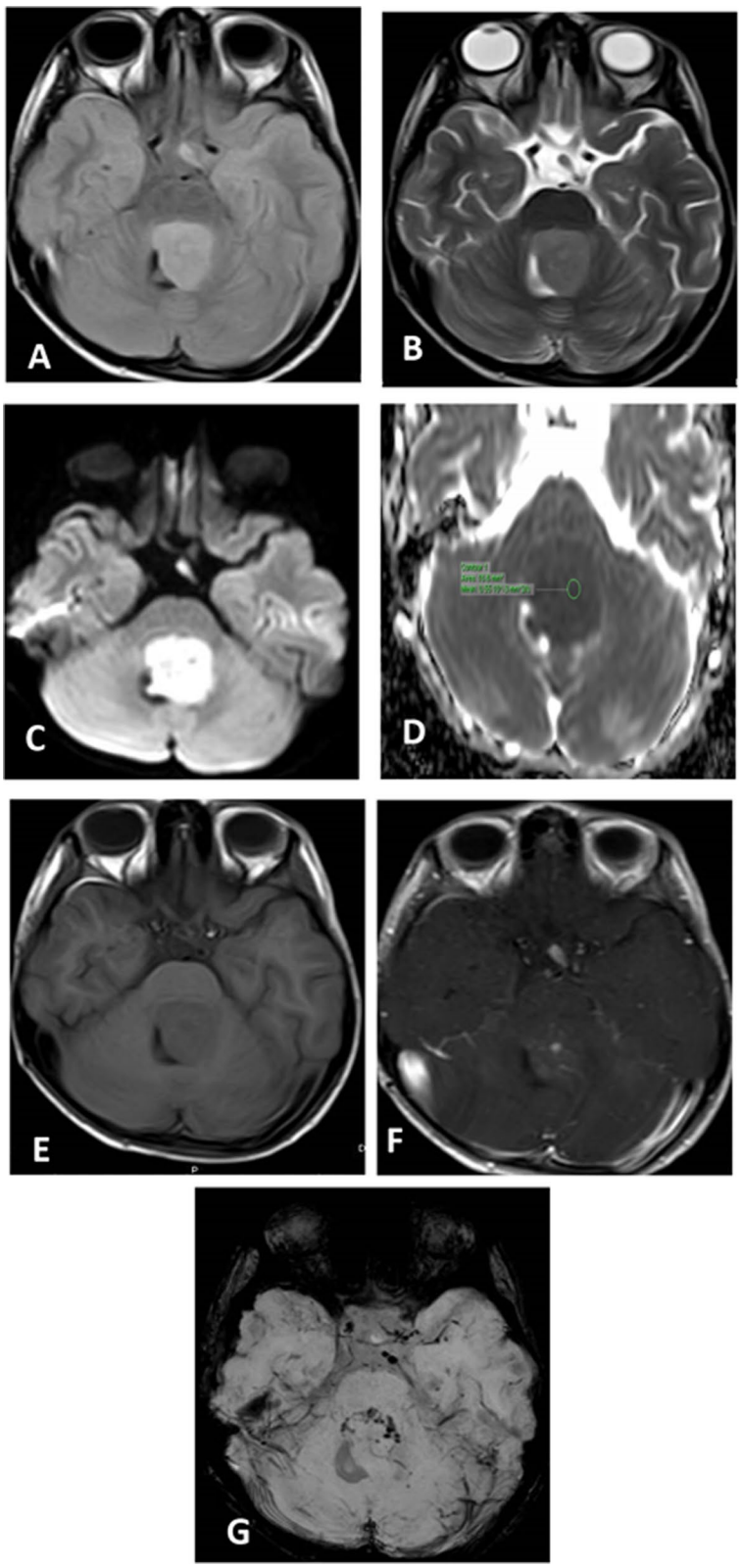

Fig. 3 A 10-year-old male child with posterior fossa medulloblastoma. **A** Axial FLAIR and **B** T2 WI show mass in the fourth ventricle of high signal. **C** Axial DWI and **D** ADC show diffusion restriction with low ADC value measuring 0.55×10^{-3} mm^2/s. **E** Axial pre-contrast T1WI shows low signal. **F** Axial post-contrast T1WI shows mild enhancement. **G** SWI shows more than 10 foci of hypointense signal (ITSS score 2)

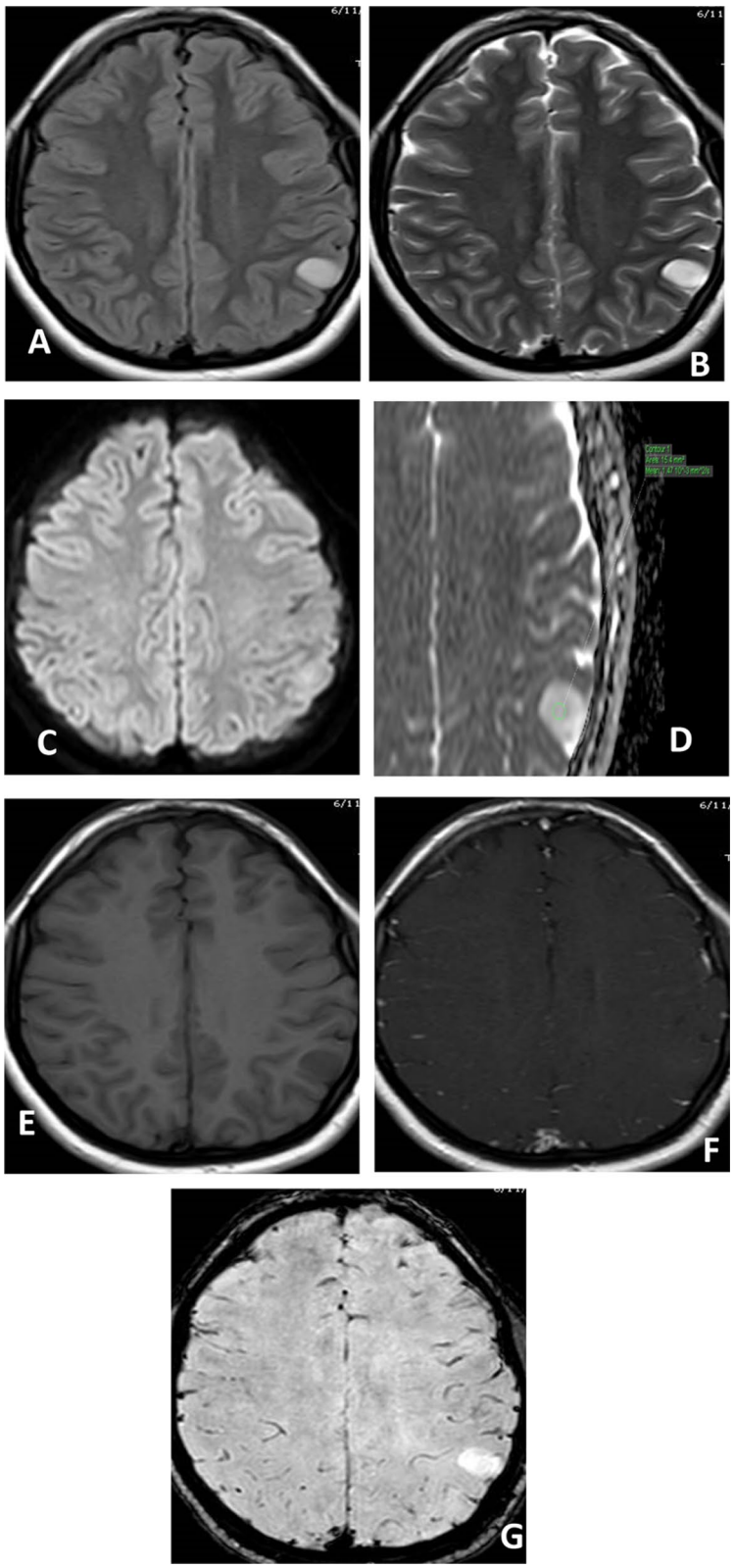

Fig. 4 A 12-year-old female child with left parietal low-grade glioma. **A** Axial FLAIR and **B** T2WI show high signal left parietal cortical space-occupying lesion. **C** Axial DWI and **D** ADC show no diffusion restriction with high ADC value measuring 1.47×10^{-3} mm^2/s. **E** Axial pre-contrast T1WI shows low signal. **F** Axial post-contrast T1WI shows no enhancement. **G** SWI shows absent hypointense signal foci (ITSS score 0)

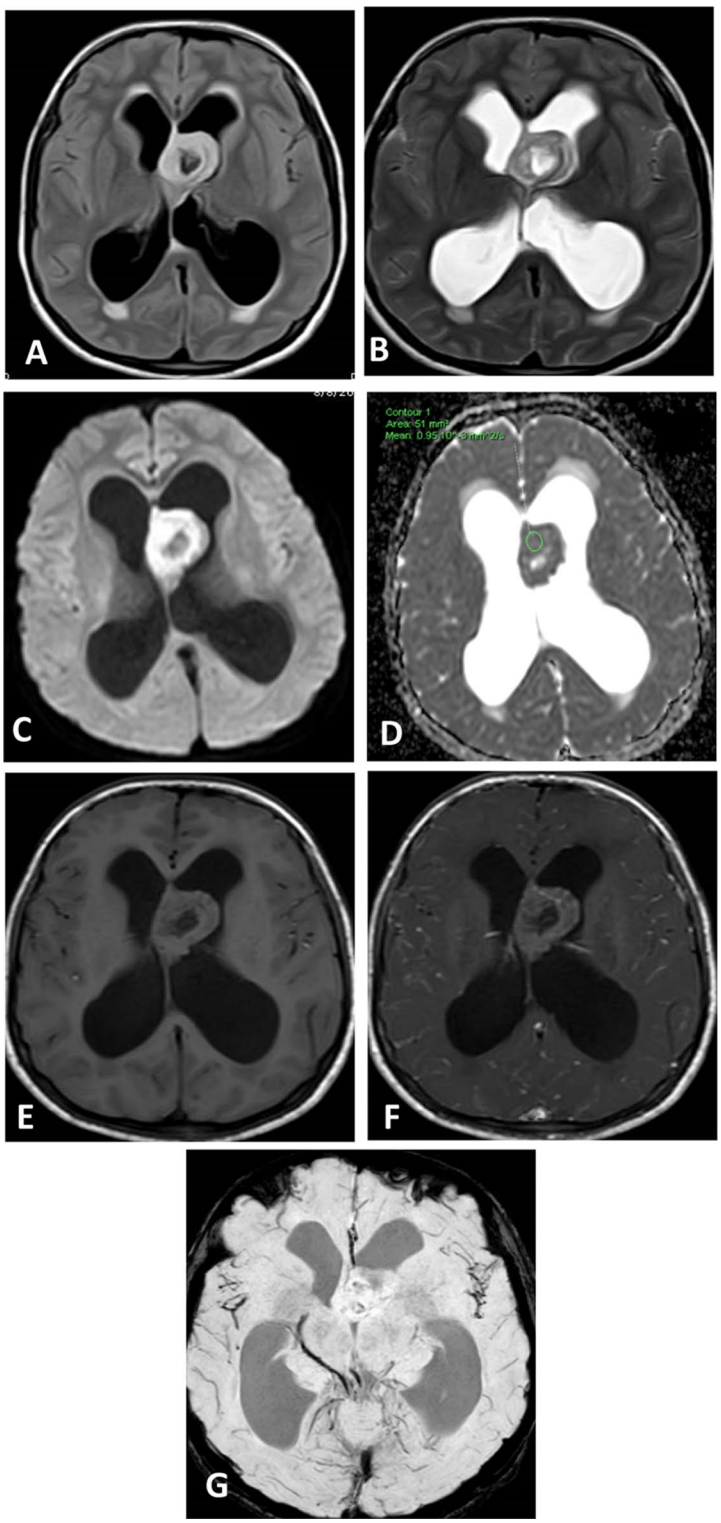

Fig. 5 A 16-year-old male child with central neurocytoma. **A** Axial FLAIR and **B** T2WI show high signal space-occupying lesion based on the septum pellucidum causing obstructive hydrocephalus. **C** Axial DWI and **D** ADC show diffusion restriction with low ADC value measuring 0.95×10^{-3} mm^2/s. **E** Axial pre-contrast T1WI shows isointense signal. **F** Axial post-contrast T1WI shows mild enhancement. **G** SWI shows more than 10 foci of hypointense signal (ITSS score 2)

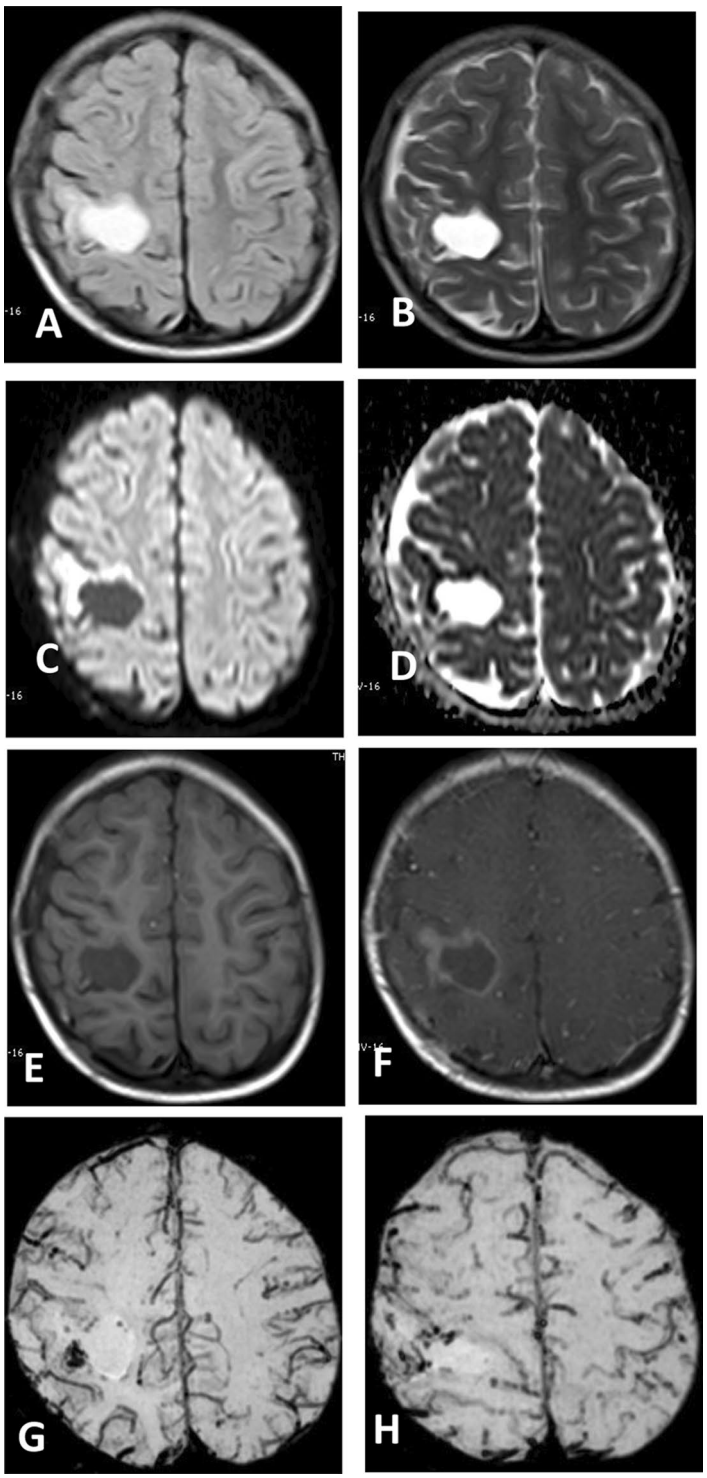

Fig. 6 A 5-year-old female child presenting with high-grade supratentorial ependymoblastoma. **A** Axial FLAIR and **B** T2WI show right high frontal space-occupying lesion of bright signal. **C** Axial DWI and **D** ADC show a rim of restricted diffusion with low ADC value measuring 0.99×10^{-3} mm^2/s. **E** Axial T1WI shows low signal mass. **F** Axial post-contrast T1WI shows rim enhancement with mural nodule along its lateral border. **G**, **H** SWI shows prominent vascularity particularity along its lateral aspect with more than 10 foci of hypointense signal (ITSS score 2)

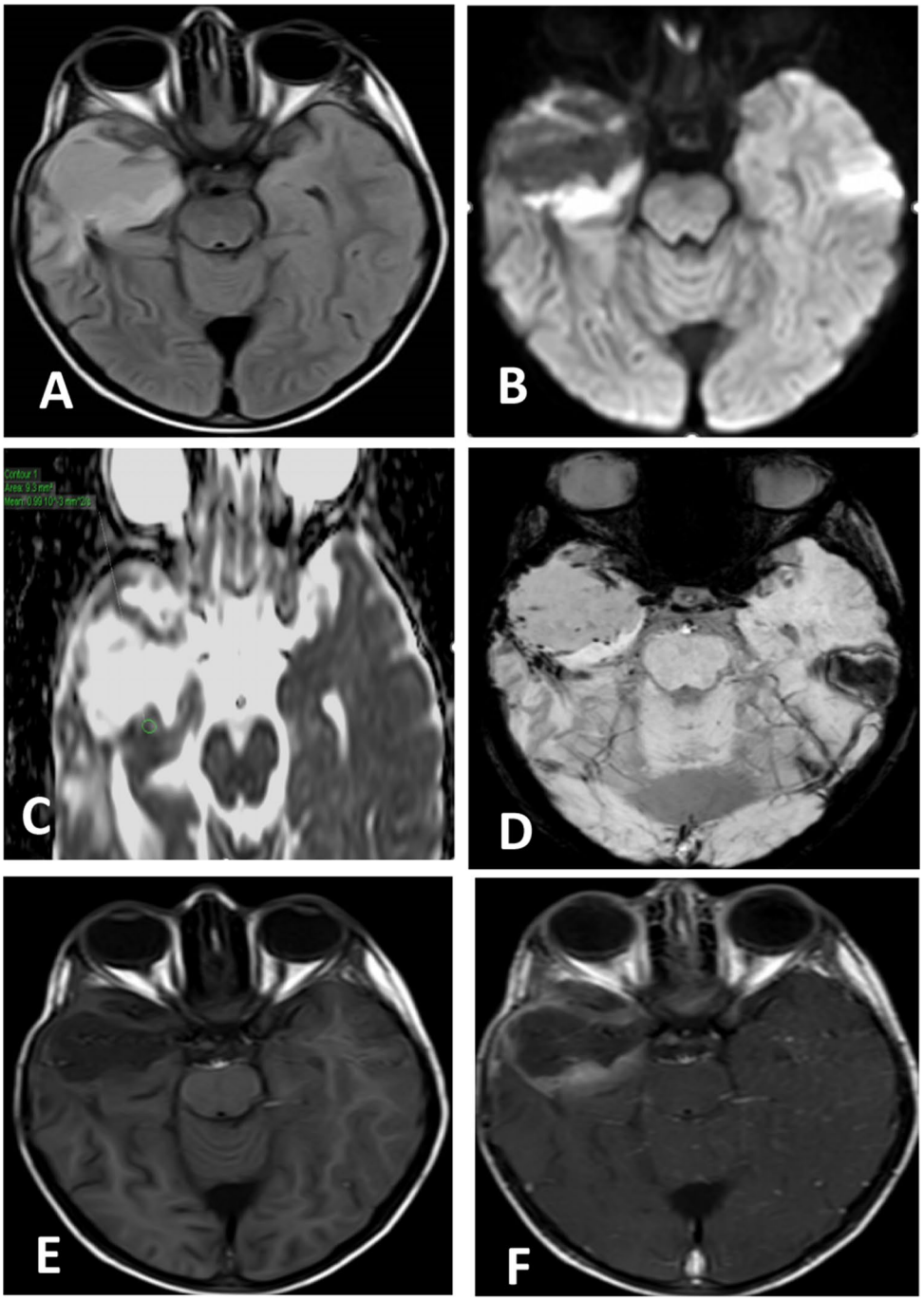

Fig. 7 Twelve-year-old female children presenting with anaplastic astrocytoma. **A** Axial FLAIR shows right temporal space-occupying lesion of intermediate signal. **B** Axial DWI and **C** ADC show diffusion restriction with low ADC value measuring 0.99×10^{-3} mm^2/s. **D** SWI shows prominent vascularity with more than 10 foci of hypointense signal (ITSS score 2). **E** Axial T1WI shows low signal mass. **F** Axial post-contrast T1WI shows peripheral enhancement

A study done by Xu et al. [15] assessing and grading gliomas used a threshold value of 1.497 for rADC with sensitivity and specificity of 86.2% and 85%, respectively, for determining high-grade gliomas. Bulakbasi et al. [28] concluded that ADC is significantly different between low-grade gliomas and high-grade gliomas. On the other hand, results by Castillo et al. [11] and Wu CC et al. [29] showed that the tumors diffusion is affected by other several factors such as tumor necrosis, sizes of pores in extracellular spaces, surrounding vasogenic edema, and not only tumor cell density; thus, differentiation between gliomas should not be based solely on the ADC or rADC.

ITSS score 2 was a positive predictor of high-grade tumors in our study, with an odds ratio of 29.812. In contrast, the rADC value was a negative predictor for high-grade tumors ($y = 10.193 + (\text{rADC} \times -6.211)$). Adding SWI and DWI to the conventional MRI study will help with tumor grading. Radiological grading of tumors using conventional and contrast-enhanced sequences alone is prone to errors, necessitating the addition of other parameters to supplement proper tumor grading and assist surgeons in targeting tumor tissues with the highest degree of malignancy for proper surgical biopsy. We recommend further clinical studies to be done to investigate the usefulness of MRI advanced sequences that are normally included in adult brain tumors protocol imaging to assess their role in pediatric brain tumor imaging and combining sequences such as SWI, DWI, and perfusion imaging studies.

Limitation

The potential limitations of this study included the small sample of patients and the higher number of high-grade lesions as compared to those of low-grade lesions. The tumor pathologies were also not equally distributed.

Conclusions

Susceptibility-weighted imaging, apparent diffusion coefficient (ADC), and relative ADC (rADC) are applicable sequences that can be easily used nowadays for non-invasive preoperative pathological grading of pediatric brain tumors, hence assisting the surgeon and oncologist for proper treatment planning. ITSS score 2 was a positive predictor of high-grade tumors in our study. We recommend further studies that include MRI combined sequences as SWI with perfusion imaging studies.

Acknowledgements
Not applicable.

Author contributions
All authors contributed to the study conception and design. Material preparation and data collection were performed by A.S.A. Image analysis was performed by N.H.K., M.E.Y.E., and A.S.A. Statistical analysis was conducted by A.S.A. Data interpretation was performed N.H.K. and M.E.Y.E. The first draft of the manuscript was written by N.H.K. and M.E.Y.E., and the manuscript was proofread by A.S.A. All authors critically revised and commented on previous versions of the manuscript. All authors read and approved the final manuscript.

Funding
This research did not receive any specific grant from funding agencies in the public, commercial, or not-for-profit sectors.

Availability of data and materials
The datasets used and/or analyzed during the current study are available from the corresponding author on reasonable request.

Declarations

Ethics approval and consent to participate
The authors are accountable for all aspects of the work in ensuring that questions related to the accuracy or integrity of any part of the work are appropriately investigated and resolved. The study was conducted in accordance with the Declaration of Helsinki (as revised in 2013). This prospective study was approved by the Research Ethics Committee of the Faculty of Medicine at Ain shams University in Egypt (FWA 000017585). Reference Number of approval: R 68/2020. A written informed consent to participate in this research was given by all children's guardians.

Consent for publication
All children's guardians gave written informed consent to publish the data contained within this study.

Competing interest
The authors declare that they have no conflicts of interest. The authors declare that they have financial or non-financial interests that are directly or indirectly related to the work submitted for publication.

Received: 6 July 2022 Accepted: 16 September 2022
Published online: 03 October 2022

References

1. Aydin O, Buyukkaya R, Hakyemez B (2017) Susceptibility imaging in glial tumor grading; using 3 tesla magnetic resonance (MR) system and 32 channel head coil. Pol J Radiol 82:179–187
2. Segal D, Karajannis MA (2016) Pediatric brain tumors: an update. Curr Probl Pediatr Adolesc Health Care 46(7):242–250
3. Tynninen O, Aronen HJ, Ruhala M et al (1999) MRI enhancement and microvascular density in gliomas. Correlation with tumor cell proliferation. Invest Radiol 34(6):427–434
4. Schad LR (2001) Improved target volume characterization in stereotactic treatment planning of brain lesions by using high-resolution BOLD MR-venography. NMR Biomed 14:478–483
5. Sehgal V, Delproposto Z, Haddar DH et al (2006) Susceptibility-weighted imaging to visualize blood products and improve tumor contrast in the study of brain masses. J Magn Reson Imaging 24(1):41–51
6. Kim HS, Jahng GH, Ryu CW et al (2009) Added value and diagnostic performance of intratumoral susceptibility signals in the differential diagnosis of solitary enhancing brain lesions: preliminary study. Am J Neuroradiol 30(8):1574–1579
7. Gaudino S, Marziali G, Pezzullo G et al (2020) Role of susceptibility-weighted imaging and intratumoral susceptibility signals in grading and differentiating pediatric brain tumors at 1.5 T: a preliminary study. Neuroradiology 62(6):705–713
8. Kong LW, Chen J, Zhao H et al (2019) Intratumoral susceptibility signals reflect biomarker status in gliomas. Sci Rep 9:17080
9. Abdelrahman AS, Abbas YA, Abdelwahab SM et al (2021) Potential role of susceptibility-weighted imaging in the diagnosis of non-neoplastic pediatric neurological diseases. Egypt J Radiol Nucl Med 52:188
10. Heiss WD, Raab P, Lanfermann H (2011) Multimodality assessment of brain tumors and tumor recurrence. J Nucl Med 52:1585–1600

11. Castillo M, Smith JK, Kwock L et al (2001) Apparent diffusion coefficients in the evaluation of high-grade cerebral gliomas. Am J Neuroradiol 22(1):60–64
12. Higano S, Yun X, Kumabe T et al (2006) Malignant astrocytic tumors: clinical importance of apparent diffusion coefficient in prediction of grade and prognosis. Radiology 241(3):839–846
13. Duy Hung N, Minh Duc N, Hong Nhung T et al (2020) The correlation between apparent diffusion coefficient (ADC) and relative cerebral blood volume (rCBV) with Ki-67 expression in central nervous system lymphoma. Int J Cancer Manag 13(12):e107834
14. Surov A, Meyer HJ, Wienke A (2017) Associations between apparent diffusion coefficient (ADC) and KI 67 in different tumors: a meta-analysis. Part 1: ADC_{mean}. Oncotarget 8(43):75434–75444
15. Xu J, Xu H, Zhang W et al (2018) Contribution of susceptibility- and diffusion-weighted magnetic resonance imaging for grading gliomas. Exp Ther Med 15(6):5113–5118
16. Hsu CC, Watkins TW, Kwan GN et al (2016) Susceptibility-weighted imaging of glioma: update on current imaging status and future directions. J Neuroimaging 26(4):383–390
17. Saini J, Gupta PK, Sahoo P et al (2018) Differentiation of grade II/III and grade IV glioma by combining "T1 contrast-enhanced brain perfusion imaging" and susceptibility-weighted quantitative imaging. Neuroradiology 60(1):43–50
18. Morana G, Alves CA, Tortora D et al (2018) T2*-based MR imaging (gradient echo or susceptibility-weighted imaging) in midline and off-midline intracranial germ cell tumors: a pilot study. Neuroradiology 60(1):89–99
19. Haddar D, Haacke E, Sehgal V et al (2004) L'imagerie de susceptibilité magnétique: théorie et applications [Susceptibility weighted imaging. Theory and applications]. J Radiol 85(11):1901–1908
20. Hori M, Mori H, Aoki S et al (2010) Three-dimensional susceptibility-weighted imaging at 3 T using various image analysis methods in the estimation of grading intracranial gliomas. Magn Reson Imaging 28(4):594–598
21. Park SM, Kim HS, Jahng GH et al (2010) Combination of high-resolution susceptibility-weighted imaging and the apparent diffusion coefficient: added value to brain tumor imaging and clinical feasibility of non-contrast MRI at 3 T. Br J Radiol 83(990):466–475
22. Rauscher A, Sedlacik J, Barth M et al (2005) Nonnvasive assessment of vascular architecture and function during modulated blood oxygenation using susceptibility weighted magnetic resonance imaging. Magn Reson Med 54(1):87–95
23. Aboian MS, Solomon DA, Felton E et al (2017) Imaging characteristics of pediatric diffuse midline gliomas with histone H3 K27M mutation. Am J Neuroradiol 38(4):795–800
24. Gaudino S, Martucci M, Russo R et al (2017) MR imaging of brain pilocytic astrocytoma: beyond the stereotype of benign astrocytoma. Childs Nerv Syst 33(1):35–54
25. Gupta PK, Saini J, Sahoo P et al (2017) Role of dynamic contrast-enhanced perfusion magnetic resonance imaging in grading of pediatric brain tumors on 3T. Pediatr Neurosurg 52(5):298–305
26. Lin H, Leng X, Qin CH et al (2019) Choroid plexus tumours on MRI: similarities and distinctions in different grades. Cancer Imaging 19(1):17
27. Sie M, de Bont ES, Scherpen FJ et al (2010) Tumour vasculature and angiogenic profile of paediatric pilocytic astrocytoma; is it much different from glioblastoma? Neuropathol Appl Neurobiol 36(7):636–647
28. Bulakbasi N, Guvenc I, Onguru O et al (2004) The added value of the apparent diffusion coefficient calculation to magnetic resonance imaging in the differentiation and grading of malignant brain tumors. J Comput Assist Tomogr 28(6):735–746
29. Wu CC, Guo WY, Chen MH et al (2012) Direct measurement of the signal intensity of diffusion-weighted magnetic resonance imaging for preoperative grading and treatment guidance for brain gliomas. J Chin Med Assoc 75(11):581–588

Publisher's Note